Bulletin of Electrical Engineering and Informatics
Vol. 13, No. 3, June 2024, pp. 1504~1512
ISSN: 2302-9285, DOI: 10.11591/eei.v13i3.5209

Speed control for traction motor of urban electrified train in field weakening region based on backstepping method

An Thi Hoai Thu Anh[1], Ngo Manh Tung[2]
[1]Department of Electrical Engineering, Faculty of Electronics-Electric, University of Transport and Communications, Hanoi, Vietnam
[2]Division of Control and Automation Engineering, Faculty of Electrical Engineering, Hanoi University of Industry, Hanoi, Vietnam

Article Info

Article history:

Received Nov 11, 2022
Revised Oct 4, 2023
Accepted Dec 21, 2023

Keywords:

Backstepping technique
Field oriented control
Field weakening control
Induction motor
Urban electric train

ABSTRACT

Tractor motors always operate in the speed region higher than rated speed, but is limited to the module of the stator current, stator voltage vectors. Additionally, mathematical model of traction motor has shown nonlinearity through the product of the state variables i_{sd}, i_{sq} with the input variable ω_s:$\omega_s i_{sq}$, $\omega_s i_{sd}$. Therefore, this paper focuses on the study of speed control of traction motors in weakening field region while optimizing torque control, and choosing the backstepping method in designing speed–flux controller in order to solve the nonlinear structure. The simulation results of the responses: speed, torque, power, and flux performed on MATLAB/Simulink software with parameters collected from metro Nhon-Hanoi Station, Vietnam have proven the correctness in theoretical research.

Corresponding Author:

An Thi Hoai Thu Anh
Department of Electrical Engineering, University of Transport and Communications
No. 3 Cau Giay Street, Lang Thuong Ward, Dong Da District, Hanoi, Vietnam
Email: htanh.ktd@utc.edu.vn

1. INTRODUCTION

With the outstanding advantages of the ability to carry a large number of passengers, safely, on time, reducing traffic congestion and pollution environment in big cities, urban electrified trains are increasingly attracted the attention from researchers and governments all over the world [1], [2]. In Vietnam, some urban railway lines have been put into operation and others are about to be operated in the near future. However, to ensure the quality of train operation, studies on traction engines are essential. Due to the great development of power electronic converters, induction motors are widely used as traction motors due to their simple structure and speed control range. The operation characteristics of traction motors used in transportation different from industrial loads, which is often operated in the speed region greater than the rated speed. However, when the control speed is higher than the rated speed, there are limitations on stator voltage and current modules, so it is imperative to control spedd in weakening flux region.

Mengoni *et al.* [3], Harnefors *et al.* [4] focused on the stator flux vector control of induction motor (IM) in the field weakening region to ensure maximum torque but ignore the requirements for maximum torque output. Son *et al.* [5] proposed a flux control method for operating IM with the condition that voltage on DC-link varies to ensure maximum output power. Zarri *et al.* [6], Abu-Rub and Koltz [7], Shin *et al.* [8], Casadei *et al.* [9] also studied IM control in weakening flux region with optimal flux selection and control methods. IM control by stator flux oriented (SFO) method with stator flux inversely proportional to motor speed. However, field oriented control method (FOC) with optimal flux levels clearly calculated as a function of machine parameters; controlled by direct torque control (DTC) method with controllers being PI. Tang and Huang [10] designed the speed control of IM in weakening field region by regulating PID parameters.

Gallegos *et al.* [11] proposed a new current controller making it easier for IM to operates smoothly and maximum torque-per-ampere (MPTA) control in weakening field region given variation of motor parameters and voltage source. Casadei *et al.* [12] presented three sensorless control schemes for IM operation in the weakening flux region with maximum torque utilizing maximum voltage and current.

Lin *et al.* [13] proposed the backstepping adaptive motion control method to determine the slip surface for the sliding controller applied in motion tracking of the mechanical transmission system. Yu *et al.* [14] control position tracking with uncertainty and load disturbance using adaptive fuzzy backstepping controller. Echeikh *et al.* [15] designed non-linear backstepping controller for five-phase induction motor drive system operating at low speed. Regaya *et al.* [16] have designed 2 steps: first step of evaluating rotor flux based on the backstepping observer and the second step determines the adaptive mechanism of the rotor resistance based on the estimated rotor flux. Kirad *et al.* [17] applied sensorless backstepping technique with kalman filter to improve performances of motor. Belkacem *et al.* [18] made comparison between backstepping and backstepping sliding mode controller for some components of vehicles to show efficiency and robustness against external disturbances and various road profile. Nguyen *et al.* [19], Do *et al.* [20] used backstepping method for IM with constraints of input and output.

However, the above works have not proposed a combination of nonlinear control methods for traction motor-IM operating in the weakening field region applied to means of transportation. Therefore, this paper presents speed control of traction motor for urban electrified train in field weakening based on backstepping technique applied to metro Nhon–Hanoi Station, Vietnam.

2. MODELING ELECTRIC TRAIN

In modeling electrified train, modeling traction motor and load very needs. The continuous state model of traction motor is designed on *dq* coordinate system, analyzing the forces that impede motion including friction, air resistance, slope resistance, and curve resistance is shown in Figure 1. Survey of parameters and forces conducted on the urban railway line from Nhon to Hanoi Station, Vietnam.

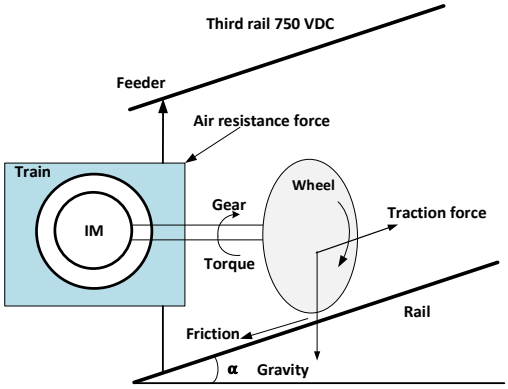

Figure 1. Forces act on train

2.1. Modeling traction motor

The traction electric motor is induction motor with the field oriented control method based on the *dq* coordinate system. The mathematical are expressed as (1) [21], [22]:

$$\begin{cases} \frac{di_{sd}}{dt} = -(\frac{1}{\sigma T_s} + \frac{1-\sigma}{\sigma T_r})i_{sd} + \omega_s i_{sq} + \frac{1-\sigma}{\sigma T_r}\psi'_{rd} + \frac{1-\sigma}{\sigma}\omega\psi'_{rq} + \frac{1}{\sigma L_s}u_{sd} \\ \frac{di_{sq}}{dt} = -(\frac{1}{\sigma T_s} + \frac{1-\sigma}{\sigma T_r})i_{sq} - \omega_s i_{sd} + \frac{1-\sigma}{\sigma T_r}\psi'_{rq} - \frac{1-\sigma}{\sigma}\omega\psi'_{rd} + \frac{1}{\sigma L_s}u_{sq} \\ \frac{d\psi_{rd}}{dt} = \frac{L_m}{T_r}i_{sd} - \frac{1}{T_r}\psi_{rd} + (\omega_s - \omega)\psi_{rq} \\ \frac{d\psi_{rq}}{dt} = \frac{L_m}{T_r}i_{sq} - (\omega_s - \omega)\psi_{rd} - \frac{1}{T_r}\psi_{rq} \\ m_M = \frac{3}{2}z_p\frac{L_m^2}{L_r}\psi'_{rd}i_{sq} = \frac{3}{2}z_p(1-\sigma)L_s\psi'_{rd}i_{sq} \\ m_M = m_L + \frac{J}{z_p}\frac{d\omega}{dt} \end{cases} \quad (1)$$

Where parameters are defined: $\psi'_{rd} = \psi_{rd}/L_m$ và $\psi'_{rq} = \psi_{rq}/L_m$; $\sigma = 1 - \frac{L_m^2}{L_s L_r}$ is leakage factor; $T_s = \frac{L_s}{R_s}$ is stator time constant; $T_r = \frac{L_r}{R_r}$ is rotor time constant; $T'_\sigma = \frac{\sigma L_\sigma}{r_\sigma}$, $\omega_s = \omega + \frac{L_m}{T_r}\frac{i_{sd}}{\psi_{rd}}$; ω is mechanical rotor speed; z_p is pairs of poles; J is torque of inertia of electric train and motor; m_L is load torque; ψ_{rd}, ψ_{rq} is rotor flux; L_m, L_r, L_s are mutual, rotor, and stator inductances respectively. Inertia torque of electric train calculated [21]:

$$J_{eq} = \frac{1}{4}\frac{M_{mas}}{N}\left(\frac{D_{wh}}{\tau}\right)^2 \quad (2)$$

where M_{mas} is mass of train, N is numbers of motors, D_{wh} is diameter of wheel, and τ is transmission ratio.

2.2. Modeling load of train

The forces impeding the movement of the train include the air resistance, the resistance due to rolling friction, which is reduced to the basic resistance by mass calculated based on the Davis formula [23]–[25]:

$$w_0 = \frac{W_0}{M_{mas}} = a + bv + cv^2 \quad (3)$$

Where *a*, *b*, *c* are the drag coefficients provided by the manufacturer and *v* is the speed of the train. Resistance due to slope:

$$F_{grad} = mg\ sin\ \alpha \quad (4)$$

Where $\sin(a) = \sin(\arctan(i_k))$, i_k (‰) is the ratio of top to bottom of the slope, α is the slope of the road, and g is the gravity.
Curve drag is calculated by (5):

$$w_r = \frac{A}{R} \quad (5)$$

With R is radius of the curve and A is coefficient determined by experiment, ranging from 450-800. With a rail gauge of 1435 mm, A=700; with a rail gauge of 1000 mm, then A=800.

3. DESIGN TRACTION MOTOR DRIVE CONTROL

The control design of the traction motor by FOC method [21] with three control loops: the current loop Ri, the flux loop R_ψ, and the speed loop R_ω demonstrated in Figure 2. In the FOC control structure, the train speed is always greater than the rated speed of the traction motor, it is necessary to control the speed within the weak-field region.

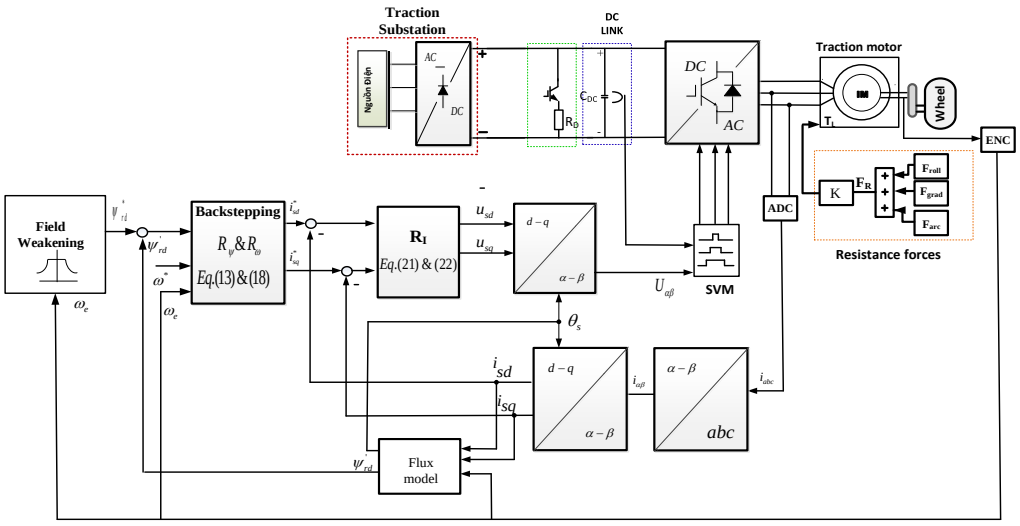

Figure 2. FOC for traction motor

3.1. Constraints of stator voltage and current in weakening field region

The two current equations of (1) show nonlinearity through the product of state variables isd, isq with input variables ω_s: $\omega_s i_{sq}$, $\omega_s i_{sd}$. Nonlinear structure features can be completely solved by nonlinear control methods. Therefore, in the control structure of the traction motor drive system, the bacstepping method chosen to design the speed and flux loop, and ψ_{rd}^* in low flux region will be performed to ensure the speed control higher than the rated speed.

Because the operating speed of the train is often greater than the rated speed of the traction motor, speed control is considered in two regions of rated flux and weakening flux corresponding to two speed regions $\omega \leq \omega_{rated}$ and $\omega > \omega_{rated}$ with the constraints of modules of stator current, voltage [21]:

$$\begin{cases} \sqrt{u_{sd}^2 + u_{sq}^2} \leq U_{smax} \\ \sqrt{i_{sd}^2 + i_{sq}^2} \leq I_{smax} \end{cases} \quad (6)$$

Stator voltage in steady state:

$$\begin{cases} u_{sd} = r_s i_{sd} - \omega_s \sigma L_s i_{sq} \\ u_{sq} = r_s i_{sq} + \omega_s L_s i_{sd} \end{cases} \quad (7)$$

The operating states leading to overvoltage all occur in the region of high frequency, so voltage drop on the resistor in (7) is smaller than that on the inductance, so it can be ignored. Substitute (7) in (6) to get:

$$\frac{i_{sd}^2}{\left(\frac{U_{max}}{\omega_s L_s}\right)^2} + \frac{i_{sq}^2}{\left(\left(\frac{U_{max}}{\omega_s \sigma L_s}\right)\right)^2} \quad (8)$$

In (8), drawing limitations of current and voltage in weakening field region in Figure 3. In Figure 3, green line is current circle, red line is voltage circle, black dashed line is the torque of the motor. It can be noticed, the higher the speed, the smaller the current i_{sd} and the motor torque will also be reduced, this is shown by the x-intersections. Figure 4 also indicated limitations of voltage u_s and currents i_s.

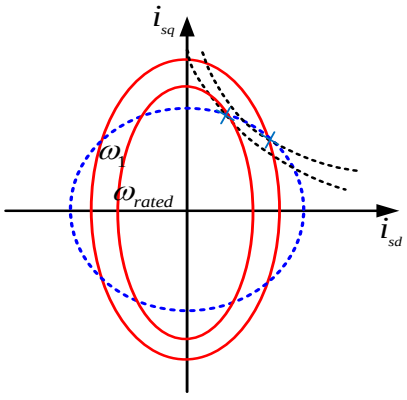

Figure 3. Limitations of current and voltage in weakening field ($\omega_{rated} < \omega_1$)

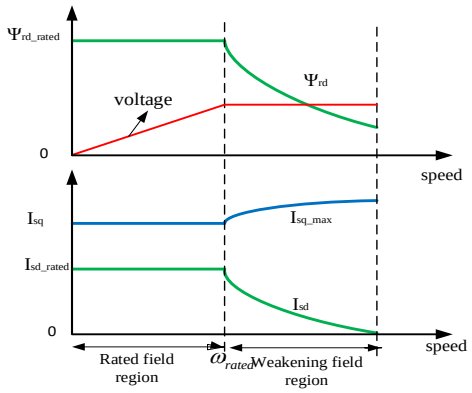

Figure 4. Rated and weakening field region

Rated speed range response in rated flux region: in this speed range even when the current is limited, the stator voltage never reaches the limitation. Under defined stator current module conditions, the two currents isd and isq must be controlled so that the working point is always at the maximum point of the torque- slip frequency curve.

Torque equation:

$$m_M = \frac{3}{2} z_p \frac{L_m^2}{L_r + L_{r\sigma}} i_{sd} i_{sq} \quad (9)$$

From (9) m_M is maximum when i_{sd}=i_{sq} and $\psi_r = \psi_{rrated} = const$

$$I_{sdN} = \frac{U_N}{\sqrt{3}\omega_{SN}L_s(I_{sdN})} \tag{10}$$

Speed range response in weakening flux region*:* in the flux attenuation range, there is an additional constraint of module of the stator voltage vector and the torque equation is calculated:

$$m_M = \frac{3}{2}z_p\frac{L_m^2}{L_r}\frac{u_{max}^2}{R_S^2}\frac{\omega_r T_r}{(\omega_r T_r+\omega_s T_s)^2+(1-\omega_s\sigma T_s\omega_r T_r)^2} \tag{11}$$

$$\psi_{rd}^* = 0{,}9i_0\frac{\omega_N}{\omega}\frac{\sqrt{3}U_{S,\max}}{U_N}\frac{L_{mN}}{L_m} \tag{12}$$

The flux characteristic in (12) is inversely proportional to the rotor angular speed, which has adapted to the fluctuations of the Udc-link voltage and to the main inductance.

3.2. Design flux and speed controller

The backstepping technique is a recursive design method applied to the system which is comprised of some nonlinear subloops. The control law and Lyapunov control function are based on the state equation in each control loop to generate the virtual control signal for the next loops. From (1), using the backstepping method synthesizes u_{sd} and u_{sq} voltage signals to the PWM.
The set values of speed and flux are ω_r^* and ψ_{rd}^*, so the errors are defined as (13):

$$\begin{cases} e_\omega = \omega_r^* - \omega_r \\ e_\psi = \psi_{rd}^* - \psi_{rd} \end{cases} \tag{13}$$

Derivative of the above system of:

$$\begin{cases} \dot{e}_\omega = \dot{\omega}_r^* - \dot{\omega}_r \\ \dot{e}_\psi = \dot{\psi}_{rd}^* - \dot{\psi}_{rd} \end{cases} \tag{14}$$

Choose Lyapunov function V_1:

$$V_1 = \frac{e_\omega^2+e_\varphi^2}{2} \tag{15}$$

Derivative V_1:

$$\dot{V}_1 = e_\omega(\dot{\omega}_r^* - \dot{\omega}_r) + e_\psi(\dot{\psi}_{rd}^* - \dot{\psi}_{rd}) \tag{16}$$

For the speeds and fluxes to approach the set value, the derivative of V_1 must be negative and take the form:

$$\dot{V}_1 = -k_1e_\omega^2 - k_2e_\psi^2 \tag{17}$$

Then the virtual control signals for the current are determined as (18):

$$\begin{cases} i_{sd}^* = \frac{T_r}{2L_m}(\dot{\psi}_{rd}^* + \frac{1}{T_r}\dot{\psi}_{rd} + k_2e_\varphi) \\ i_{sq}^* = \frac{2JL_r}{3z_p^2L_m\psi_{rd}}(\omega_r^* + \frac{z_p}{J}m_L + k_1e_\omega) \end{cases} \tag{18}$$

Where k_1 and k_2 are positive coefficients.

The virtual control signal value is the set value for the next control loop. The errors of the currents are written as (19):

$$\begin{cases} e_{i_d} = i_{sd}^* - i_{sd} \\ e_{i_q} = i_{sq}^* - i_{sq} \end{cases} \tag{19}$$

The derivative of the system of (8) combined with (1):

$$\begin{cases} \dot{e}_{i_d} = i_{sd}^* - i_{sd} = i_{sd}^* - (\frac{1}{\sigma T_s} + \frac{1-\sigma}{\sigma T_r})i_{sd} + \omega_s i_{sq} + \frac{1-\sigma}{\sigma T_r}\frac{1}{L_m}\psi_{rd} + \frac{1-\sigma}{\sigma}\omega\frac{1}{L_m}\psi_{rq} + \frac{1}{\sigma L_s}u_{sd} \\ \dot{e}_{i_q} = i_{sq}^* - i_{sq} = i_{sq}^* - (\frac{1}{\sigma T_s} + \frac{1-\sigma}{\sigma T_r})i_{sq} - \omega_s i_{sd} + \frac{1-\sigma}{\sigma T_r}\psi_{rq} - \frac{1-\sigma}{\sigma}\omega\frac{1}{L_m}\psi_{rd} + \frac{1}{\sigma L_s}u_{sq} \end{cases} \tag{20}$$

Combining (7) and (8):

$$\begin{cases} e_{i_d} = \frac{T_r}{2L_m}(\dot{\psi}^*_{rd} + \frac{1}{T_r}\dot{\psi}_{rd} + k_2 e_\psi) - i_{sd} \\ e_{i_q} = \frac{2JL_r}{3z_p^2 L_m \psi_{rd}}(\omega^*_r + \frac{z_p}{J} m_L + k_1 e_\omega) - i_{sq} \end{cases} \quad (21)$$

Choose the Lyapunov function V_2 as (22):

$$V_1 = \frac{e_\omega^2 + e_\psi^2 + e_{i_d}^2 + e_{i_q}^2}{2} \quad (22)$$

Taking the derivative of V_2:

$$\dot{V}_2 = -k_1 e_\omega^2 - k_2 e_\psi^2 - k_3 e_{i_d}^2 - k_4 e_{i_q}^2 + e_{i_d}(k_3 e_{i_d} + i^*_{sd} - ((\frac{1}{\sigma T_s} + \frac{1-\sigma}{\sigma T_r})i_{sd} + \omega_s i_{sq} + \frac{1-\sigma}{\sigma T_r}\frac{1}{L_m}\psi_{rd} + \frac{1-\sigma}{\sigma}\omega\frac{1}{L_m}\psi_{rq} + \frac{1}{\sigma L_s}u_{sd})) + e_{i_q}(k_4 e_{i_q} + i^*_{sq} - ((\frac{1}{\sigma T_s} + \frac{1-\sigma}{\sigma T_r})i_{sq} - \omega_s i_{sd} + \frac{1-\sigma}{\sigma T_r}\psi_{rq} - \frac{1-\sigma}{\sigma}\omega\frac{1}{L_m}\psi_{rd} + \frac{1}{\sigma L_s}u_{sq}) \quad (23)$$

Where k_3 and k_4 are positive coefficients.
For the Lyapunov function to have a negative value, from (12):

$$k_3 e_{i_d} + i^*_{sd} - ((\frac{1}{\sigma T_s} + \frac{1-\sigma}{\sigma T_r})i_{sd} + \omega_s i_{sq} + \frac{1-\sigma}{\sigma T_r}\frac{1}{L_m}\psi_{rd} + \frac{1-\sigma}{\sigma}\omega\frac{1}{L_m}\psi_{rq} + \frac{1}{\sigma L_s}u_{sd})) = 0 \; k_4 e_{i_q} + i^*_{sq} - ((\frac{1}{\sigma T_s} + \frac{1-\sigma}{\sigma T_r})i_{sq} - \omega_s i_{sd} + \frac{1-\sigma}{\sigma T_r}\psi_{rq} - \frac{1-\sigma}{\sigma}\omega\frac{1}{L_m}\psi_{rd} + \frac{1}{\sigma L_s}u_{sq}) = 0 \quad (24)$$

From (13) determine the control voltage signals of the system:

$$u_{sd} = \sigma L_s(k_3 e_{i_d} + i^*_{sd} - ((\frac{1}{\sigma T_s} + \frac{1-\sigma}{\sigma T_r})i_{sd} + \omega_s i_{sq} + \frac{1-\sigma}{\sigma T_r}\frac{1}{L_m}\psi_{rd} + \frac{1-\sigma}{\sigma}\omega\frac{1}{L_m}\psi_{rq})) \; u_{sq} = \sigma L_s(k_4 e_{i_q} + i^*_{sq} - ((\frac{1}{\sigma T_s} + \frac{1-\sigma}{\sigma T_r})i_{sq} - \omega_s i_{sd} + \frac{1-\sigma}{\sigma T_r}\psi_{rq} - \frac{1-\sigma}{\sigma}\omega\frac{1}{L_m}\psi_{rd})) \quad (25)$$

Where k_3 and k_4 need to be corrected to ensure that the kinetic characteristics of the current converge faster than those of the speed and the flux.

4. SIMULATION RESULTS

Simulation parameters of train, traction motors which are collected from Metro line Nhon-Hanoi Station, Vietnam including 12 stations with 12.5 km in length in which 8.5 km elevated and 4 km underground have been shown in Tables 1 and 2.

Table 1. Parameters

Parameters of train	Unit	Quality
Mass of train at full load (M)	kg	192000
Numbers of motors (N)		12
Maximum speed (vmax)	km/h	80
Base speed (vb)	km/h	40
Maximum acceleration	m/s^2	1
Coefficient a		0.0115070
Coefficient b		0.0003494
Coefficient c		0.00005497
Wheel diameter (Dwh)	m	0.84
Transmission ratio (i)		5.67:1
Gearbox performance (η_{mech})		0.85
Motor performance (η_{em})		0.95
Inertia moment of train (Jeq)	kg.m^2	87.67

Table 2. Parameters of traction motor

Parameters	Unit	Value
Rated power (P)	kW	185
Rated voltage (Un)	V	525
Number of pole pairs (z_p)		2
Rated speed (n)	revolution/minute	1485
Inertia moment (J)	kg/m^2	4.2
Stator resistance (Rr)	Ω	0.0127
Rotor resistance (Rs)	Ω	0.0127
Stator inductance (Ls)	Ω	0.0109
Rotor inductance (Lr)	Ω	0.0109
DC-link voltage (Udc)	V	1000
Total inertia torque (J)	kg.m^2	91.87

Simulation results were conducted for trains running between two stations: Kim Ma-Cat Linh with the distance of 1508 m including 3 phases: accelerating, holding, and accelerating. In which, running time of 92.2 s, train speed up to 45 km/h: acceleration time t=15.46 s, distance S=99.84 m; holding running time t=65.68 s, distance S=1337.46 m; braking time t=11.06 s, distance S=70.7 m in Figure 5.

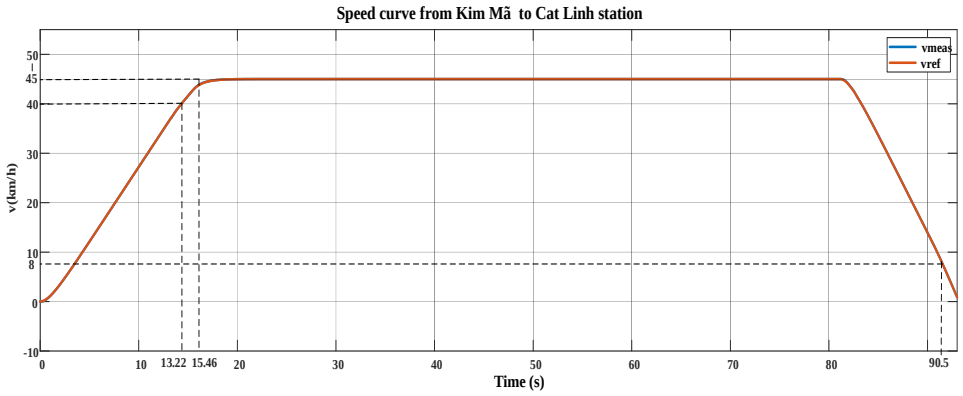

Figure 5. Response of speed curve

Figure 6 shows response of consumption power: the train mobilizes the maximum capacity from 0 to 13.22 s; from second 13.22th to second 15.46th having the constant power, hyperbolic torque corresponding to the motor operating in the weakening flux region; from second 15th to second 81th, the power consumption decreases corresponding to the train running at steady speed. After second 81th, the negative power shows that the energy is returned to the grid corresponding to the train running during the braking.

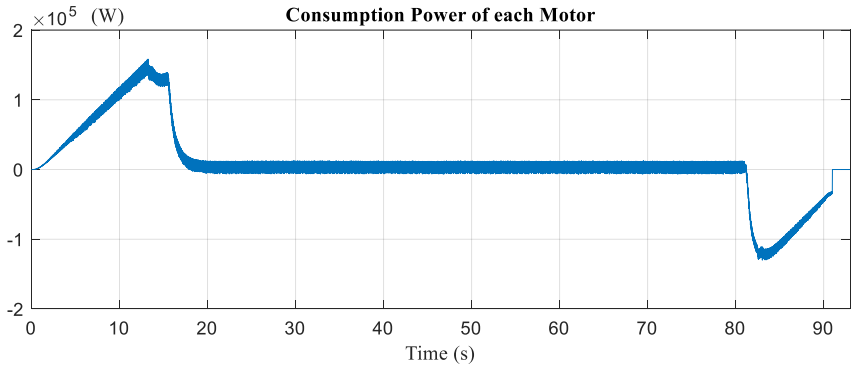

Figure 6. Consumption power of a traction motor

Figures 7 and 8, from second 13.22 th to second 15.46 th shows the period of weakening flux and torque when motor speed is greater than rated speed. This is a distinctive feature of electric train loads compared to other types of loads in the industry. In the holding phase, the torque decreases, while braking phase, negative torque indicates the regenerative braking process, where energy is returned to the grid.

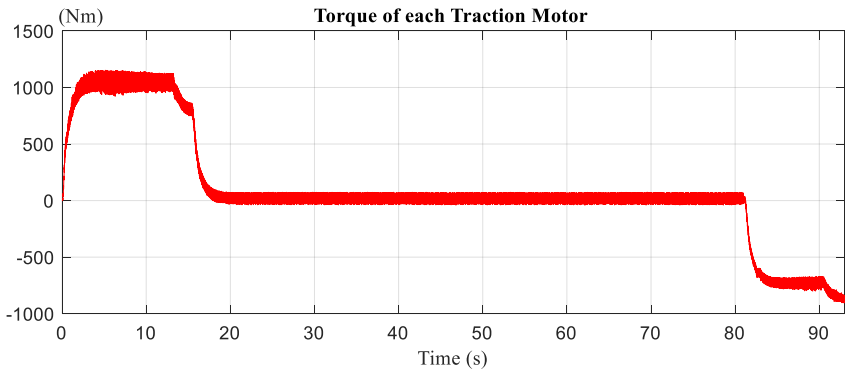

Figure 7. Torque of a traction motor

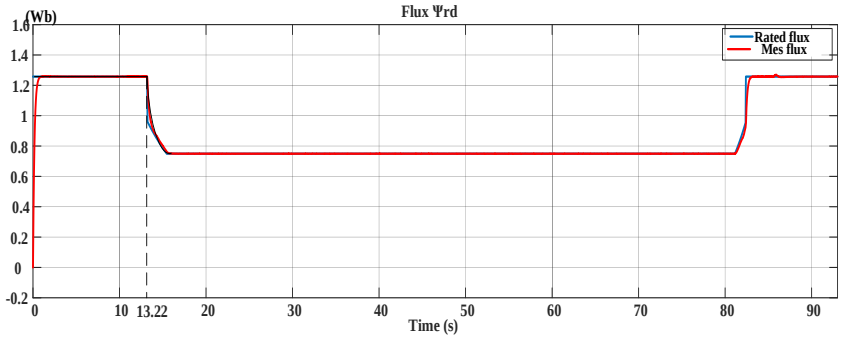

Figure 8. Response of flux

5. CONCLUSION

When urban trains operate during the acceleration phase at speeds greater than 40 km/h, it is often preferred to control the traction motor in the weak-field region to increase the train's speed while still ensuring maximum torque control. Therefore, this paper proposes to control the speed of traction motor in weakening field region with the constraints of stator voltage, current modules, using backstepping technique with simulation parameters collected from Metro Nhon–Ha Noi Station. The simulation results have shown the responses of train speed, flux, power, and torque are completely consistent with 3 train operating modes: accelerating mode, holding mode, and braking mode.

ACKNOWLEDGEMENTS

We would like to thank the financial support from University of Transport and Communications, and Hanoi University of Industry.

REFERENCES

[1] A. T. H. T. Anh and N. V. Quyen, "Optimal Speed Profile Determination with Fixed Trip Time in the Electric Train Operation of the Cat Linh-Ha Dong Metro Line based on Pontryagin's Maximum Principle," *Engineering, Technology and Applied Science Research*, vol. 10, no. 6, pp. 6488–6493, 2020, doi: 10.48084/etasr.3856.

[2] A. T. H. T. Anh and N. V. Quyen, "Energy-efficient speed profile: an optimal approach with fixed running time," *Telkomnika (Telecommunication Computing Electronics and Control)*, vol. 20, no. 3, pp. 663–671, Jun. 2022, doi: 10.12928/TELKOMNIKA.v20i3.19525.

[3] M. Mengoni, L. Zarri, A. Tani, G. Serra, and D. Casadei, "Stator flux vector control of induction motor drive in the field weakening region," *IEEE Transactions on Power Electronics*, vol. 23, no. 2, pp. 941–949, Mar. 2008, doi: 10.1109/TPEL.2007.915636.

[4] L. Harnefors, K. Pietilainen, and L. Gertmar, "Torque-maximizing field-weakening control: design, analysis, and parameter selection," in *IEEE Transactions on Industrial Electronics*, vol. 48, no. 1, pp. 161-168, Feb. 2001, doi: 10.1109/41.904576.

[5] Y. D. Son, J. H. Jung, and J. M. Kim, "Advanced field weakening control for squirrel-cage induction motor in wide range of DC-link voltage conditions," *Journal of Electrical Engineering and Technology*, vol. 12, no. 2, pp. 665–673, Mar. 2017, doi: 10.5370/JEET.2017.12.2.665.

[6] L. Zarri, M. Mengoni, A. Tani, G. Serra, D. Casadei, and J. O. Ojo, "Control schemes for field weakening of induction machines: A review," in *Proceedings - 2015 IEEE Workshop on Electrical Machines Design, Control and Diagnosis, WEMDCD 2015*, IEEE, Mar. 2015, pp. 146–155, doi: 10.1109/WEMDCD.2015.7194523.

[7] H. Abu-Rub and J. Koltz, "Rotor oriented nonlinear control system of induction motors operating at field weakening," *IECON Proceedings (Industrial Electronics Conference)*, pp. 1085–1090, 2007, doi: 10.1109/IECON.2007.4459921.

[8] M. H. Shin, D. S. Hyun, and S. B. Cho, "Maximum torque control of stator-flux-oriented induction machine drive in the field-weakening region," *IEEE Transactions on Industry Applications*, vol. 38, no. 1, pp. 117–122, 2002, doi: 10.1109/28.980365.

[9] D. Casadei, G. Serra, A. Tani, and L. Zarri, "A robust method for flux weakening operation of DTC induction motor drive with on-line estimation of the break-down torque," *2005 European Conference on Power Electronics and Applications*, vol. 2005, 2005, doi: 10.1109/epe.2005.219305.

[10] G. Tang and T. Huang, "Research on Weakening Control of Asynchronous Motor with Load Based on Vector Control," *2nd International Conference on Electrical Engineering and Automation (ICEEA) Atlantis Press*, vol. 139, pp. 103–106, 2018, doi: 10.2991/iceea-18.2018.23.

[11] G. Gallegos-López, F. S. Gunawan, and J. E. Walters, "Current control of induction machines in the field-weakened region," *IEEE Transactions on Industry Applications*, vol. 43, no. 4, pp. 981–989, 2007, doi: 10.1109/TIA.2007.900459.

[12] D. Casadei, M. Mengoni, G. Serra, A. Tani, and L. Zarri, "Field-weakening control schemes for high-speed drives based on induction motors: A comparison," *PESC Record - IEEE Annual Power Electronics Specialists Conference*, pp. 2159–2166, 2008, doi: 10.1109/PESC.2008.4592262.

[13] S. K. Lin, C. H. Fang, M. P. Chen, and J. K. Chen, "Adaptive backstepping motion control of induction motor drives," *IFAC Proceedings Volumes (IFAC-PapersOnline)*, vol. 15, no. 1, pp. 247–252, 2002, doi: 10.3182/20020721-6-es-1901.01594.

[14] J. Yu, B. Chen, and H. Yu, "Position tracking control of induction motors via adaptive fuzzy backstepping," *Energy Conversion and Management*, vol. 51, no. 11, pp. 2345–2352, Nov. 2010, doi: 10.1016/j.enconman.2010.04.008.

[15] H. Echeikh, R. Trabelsi, A. Iqbal, N. Bianchi, and M. F. Mimouni, "Non-linear backstepping control of five-phase IM drive at low speed conditions–experimental implementation," *ISA Transactions*, vol. 65, pp. 244–253, Nov. 2016, doi: 10.1016/j.isatra.2016.06.013.
[16] C. B. Regaya, F. Farhani, A. Zaafouri, and A. Chaari, "A novel adaptive control method for induction motor based on Backstepping approach using dSpace DS 1104 control board," *Mechanical Systems and Signal Processing*, vol. 100, pp. 466–481, Feb. 2018, doi: 10.1016/j.ymssp.2017.07.017.
[17] A. Kirad, S. Grouni, and Y. Soufi, "Improved sensorless backstepping controller using extended Kalman filter of a permanent magnet synchronous machine," *Bulletin of Electrical Engineering and Informatics*, vol. 11, no. 2, pp. 658–671, Apr. 2022, doi: 10.11591/eei.v11i2.3560.
[18] M. Belkacem, K. Z. Meguenni, and I. K. Bousserhane, "Comparative study between backstepping and backstepping sliding mode controller for suspension of vehicle with a magneto-rheological damper," *International Journal of Power Electronics and Drive Systems*, vol. 13, no. 2, pp. 689–704, 2022, doi: 10.11591/ijpeds.v13.i2.pp689-704.
[19] T. L. Nguyen, T. H. Vo, and N. D. Le, "Backstepping Control for Induction Motors with Input and Output Constraints," *Engineering, Technology and Applied Science Research*, vol. 10, no. 4, pp. 5998–6003, Aug. 2020, doi: 10.48084/etasr.3680.
[20] T. D. Do, N. D. Le, V. H. Phuong, and N. T. Lam, "Implementation of FOC algorithm using FPGA for GaN-based three phase induction motor drive," *Bulletin of Electrical Engineering and Informatics*, vol. 11, no. 2, pp. 636–645, Apr. 2022, doi: 10.11591/eei.v11i2.3569.
[21] N. P. Quang and J. A. Dittrich, "Vector Control of Three-Phase AC Machines: System Development in the Practice," *Power Systems*, vol. 20, 2008.
[22] M. Quraan and J. Siam, "Modeling and simulation of railway electric traction with vector control drive," in *2016 IEEE International Conference on Intelligent Rail Transportation, ICIRT 2016*, IEEE, Aug. 2016, pp. 105–110, doi: 10.1109/ICIRT.2016.7588718.
[23] N. D. T. D. D. Tuan, "Developing a program to calculate the unitresultant force of trains on Vietnam railways," *Transport and Communications Science Journal*, vol. 71, no. 8, pp. 907–923, 2020.
[24] N. V. Tiem, "Speed control for the train of urban railway using fuzzy-d controller," *Transport and Communications Science Journal*, vol. 71, no. 6, pp. 640–650, 2020.
[25] N. D. K. T. V. Khoi, "Optimal planning of substations on urban railway power supply systems using integer linear programming," *Transport and Communications Science Journal*, vol. 70, no. 4, pp. 264–278, 2019.

BIOGRAPHIES OF AUTHORS

An Thi Hoai Thu Anh received her Engineer (1997), M.Sc. (2002) degrees in Industrial Automation Engineering from Hanoi University of Science and Technology, and completed Ph.D. degree in 2020 from University of Transport and Communications (UTC). Now, she is a lecturer of Faculty of Electrical and Electronic Engineering under University of Transport and Communications (UTC). Her current interests include power electronic converters, electric motor drive, and saving energy solutions applied for industry and transportation. She can be contacted at email: htanh.ktd@utc.edu.vn.

Ngo Manh Tung Ngo Manh Tung is currently a lecturer at the Faculty of Electrical Engineering-Hanoi University of Industry. He received his B.Sc. (2011), M.Sc. (2013) majoring in Industrial Automation Engineering and completing the Ph.D. program in control and automation at Hanoi University of Science and Technology in 2022. Research direction: motor control and motion control. He can be contacted via email: tung_nm@haui.edu.vn.